Photoexcitation and Electron Transfer Properties of Rod- and Coil-Type Oligo(thienylene−ethynylene)s

Mamoru Fujitsuka,[‡] Takashi Makinoshima,[‡] Osamu Ito,*[,‡] Yuko Obara,[†] Yoshio Aso,[†] and Tetsuo Otsubo*[,†]

Institute of Multidisciplinary Research for Advanced Materials, Tohoku University, Katahira, Aoba-ku, Sendai 980-8577, Japan, and Department of Applied Chemistry, Faculty of Engineering, Hiroshima University, Higashi-Hiroshima 739-8527, Japan

Received: October 11, 2002; In Final Form: November 19, 2002

Photoexcitation and electron-transfer properties of two series of oligo(thienylene−ethynylene)s, in which thiophene rings were connected with ethynylene groups at 2,5 or 2,3 positions (*n*αTE or *n*βTE; *n* denotes the number of the repeating unit), have been studied. From MO calculations and steady-state absorption spectra, expanded π-electron systems were expected for rod-type *n*αTE in the ground states, while limited π-electron systems were expected for coil-type *n*βTE. On the other hand, because *n*βTE shows a substantial red shift of the fluorescence band similar to that of *n*αTE with increasing *n* value, a conformational change expanding π-conjugation of *n*βTE was suggested in the excited state. From the picosecond laser flash photolysis, the time scale for the conformational change was evaluated to be ca. 30 ps. The triplet state properties of *n*αTE and *n*βTE were estimated by means of the nanosecond laser flash photolysis. Furthermore, electron donor abilities of the present oligomers were investigated by studying the photoinduced electron-transfer processes with fullerenes, C_{60} and C_{70}. It was revealed that the present oligomers donate an electron to the triplet excited C_{60} or C_{70} generating the radical cations and anions of oligomers and fullerene, respectively. The electron-transfer rate constants were as small as 0.07−0.0008 of the diffusion-controlled limit, indicating the longer range electron-transfer processes due to larger size of the oligomers and fullerenes. On the other hand, back-electron-transfer processes proceeded at the diffusion-limiting rate.

Introduction

In the field of nanostructured materials, organic conducting materials attracted much attention. For this purpose, oligomers of π-conjugated polymers seem to be promising candidates.[1,2] To date, various kinds of oligomers have been investigated as molecular wires.[2] Oligo(2,5-thienyl)s, that is, homo-oligothiophenes, have been the most investigated conducting oligomers.[3] Their photophysical and photochemical properties have been investigated by means of nano- and picosecond laser flash photolysis studies.[3−9] Photoinduced electron-transfer processes of homo-oligothiophenes have been known with various acceptors, such as viologen, tetracyanoethylene, nitro compounds, and fullerenes.[4−8] Their oxidized states have been successfully observed in the transient absorption spectroscopy.[4−8]

On the other hand, studies on the conducting oligomers of copolymers seem to be few.[10] Especially, little has been known on their photophysical and photochemical properties. The small number of the investigations on the oligomers of copolymers may be attributed to difficulty in synthesizing well-controlled structures with heterocoupling reactions, while a wide variety of the materials and interesting properties are expected for the oligomers including ethene or ethyne groups or both, as well as heterocyclic rings.

In the present study, we examined photoexcitation and electron-transfer properties of two series of oligo(thienylene−ethynylene)s (Chart 1), in which thiophene rings were connected with ethynylene groups at 2,5 or 2,3 positions (*n*αTE or *n*βTE, *n* denotes the number of the repeating unit), showing rod- and coil-type structures, respectively. These oligomers have been synthesized recently,[11] and interesting properties are expected depending on their chemical structure in both the ground and excited states. By means of steady-state and transient absorption studies, their conjugation properties are revealed. Furthermore, their electron donor abilities are investigated by studying the photoinduced electron-transfer processes with fullerenes (C_{60}

CHART 1

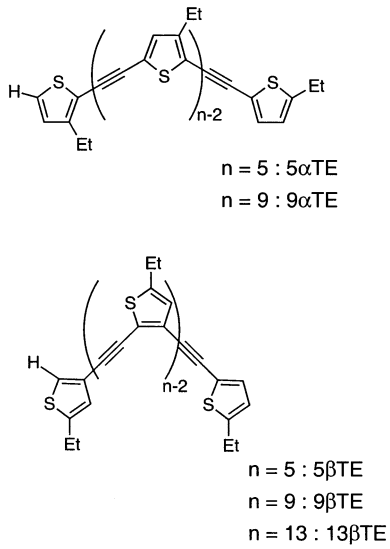

[‡] Tohoku University.
[†] Hiroshima University.

10.1021/jp027198p CCC: $25.00
Published on Web 12/17/2002

and C_{70}), which are known to show excellent acceptor abilities in the triplet excited states to homo-oligothiophenes.[8c] The effects of size of oligomers are discussed on the basis of the estimated rate constants.

Experimental Section

Materials. Syntheses of *n*αTE and *n*βTE were described in the previous papers.[11] Other chemicals were of the best commercial grade available.

Apparatus. The subpicosecond transient absorption spectra were observed by the pump and probe method. The samples were excited with a second harmonic generation (SHG, 388 nm) of output from a femtosecond Ti:sapphire regenerative amplifier seeded by SHG of an Er-doped fiber laser (Clark-MXR CPA-2001 plus, 1 kHz, fwhm 150 fs). The excitation light was depolarized. A white continuum pulse generated by focusing the fundamental light on a flowing H_2O cell was used as a monitoring light. The visible monitoring light transmitted through the sample was detected with a dual MOS detector (Hamamatsu Photonics, C6140) equipped with a polychromator (Acton Research, SpectraPro 150). The spectra were obtained by averaging on a microcomputer.[12]

Nanosecond transient absorption measurements were carried out using a Nd:YAG laser. For selective excitation of the samples, output of an OPO laser (Continuum Surelite OPO and Surelite II-10) was employed as an excitation source. For short time scale measurements (<2 μs), probe light from a pulsed Xe lamp was detected with a Ge-avalanche photodiode equipped with a monochromator after passing through the sample in quartz cell (1 cm $\times$ 1 cm). Long time scale phenomena (>2 μs) were observed by using a continuous Xe lamp as probe light. Sample solutions were deaerated by bubbling Ar gas through the solutions for 15 min. Details of the transient absorption measurements were described in our previous papers.[8c,12]

Steady-state fluorescence spectra of the samples were measured on a Shimadzu RF-5300PC spectrofluorophotometer. Fluorescence spectra in the near-IR region were measured using an argon-ion laser (Spectra-Physics, BeamLok 2060-10-SA, 514 nm, ca. 200 mW) as an excitation source. The emission from the sample was focused on to a monochromator (Koken Kogyo, SG-100) equipped with an InGaAs-PIN photodiode (New Focus, 2153). The output signal was recorded using a lock-in amplifier (NF Electronic Instruments, LI 5640).

Fluorescence lifetimes were measured by a single-photon counting method using a streakscope (Hamamatsu Photonics, C4334-01). The samples were excited with a SHG (410 nm) of a Ti:sapphire laser (Spectra-Physics, Tsunami 3950-L2S, fwhm 1.5 ps) equipped with a pulse selector (Spectra-Physics, 3980) and a harmonic generator (Spectra-Physics, GWU-23PS).

Steady-state absorption spectra in the visible and near-IR regions were measured on a Jasco V530 spectrophotometer. γ-Ray radiolysis of oligomers in *n*-butyl chloride matrix at 77 K was carried out at 2.4×10^4 R h^{-1} for 24 h.

Electrochemical measurements were carried out using a BAS CV50W voltammetric analyzer in a conventional three-electrode cell equipped with Pt working and counter electrodes with a Ag/Ag^+ reference electrode at scan rate of 100 mV/s. In each case, solution contains 0.1 mM sample with 0.1 M tetrabutylammonium perchlorate and is deaerated with Ar bubbling before measurements.

Theoretical Calculations. All calculations were made using Gaussian 98.[13] Geometry optimization and calculations of molecular orbital coefficients were performed using the semiempirical PM3 method.

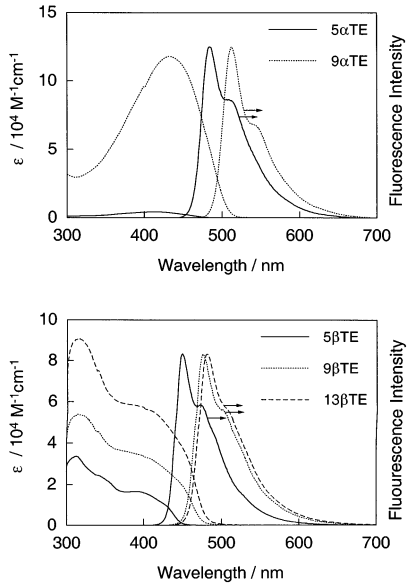

Figure 1. Absorption and fluorescence spectra of (upper panel) 5αTE and 9αTE and (lower panel) 5βTE, 9βTE, and 13βTE in toluene. Fluorescence intensities are normalized.

TABLE 1: Singlet, Triplet, and Oxidation State Properties of Oligo(thienylene−ethynylene)s[a]

	5αTE	9αTE	5βTE	9βTE	13βTE
$\lambda_{max}(S_0-S_n)$, nm	412	433	313	314	317
$\lambda_{max}(S_1-S_0)$, nm	484	512	449	475	481
τ_F, ns	0.30	0.33	0.76	0.70	0.79
$\lambda_{max}(S_1-S_n)$, nm	>900, 720	>900	>900, 587	660	700
$\lambda_{max}(T_1-T_n)$, nm	720	820	780	840	900
τ_T, μs	23	16	23	32	24
k_{TT}, M^{-1} s^{-1}	1.1×10^9	1.6×10^9	1.4×10^9	2.5×10^9	1.8×10^9
Φ_{ISC}	0.50	0.72	0.13	0.54	0.65
$E_{ox}(n\text{TE}^{\bullet+}/n\text{TE})$[b]	0.88	0.74	0.84	0.72	0.69
$\lambda_{max}(n\text{TE}^{\bullet+})$, nm[c]	1800, 740	>2000, 770	668	688	*d*

[a] In toluene. [b] The values (V vs Ag/Ag^+) were estimated in benzonitrile including 0.1 M tetrabutylammonium perchlorate as a supporting electrolyte. [c] The absorption spectra were observed after γ-ray radiolysis in *n*-butyl chloride at 77 K. [d] Observation was difficult due to lower solubility of the sample.

Results and Discussions

Ground-State Properties and MO of *n*αTE and *n*βTE. Steady-state absorption spectra of *n*αTE and *n*βTE are shown in Figure 1. In the case of *n*αTE, the absorption peak (λ_{max}-(S_0-S_n) in Table 1) shows a shift to the longer wavelength side with increasing *n* value; that is, 5αTE and 9αTE show absorption maxima at 412 and 433 nm, respectively. The findings indicate that the π-conjugation is extended in the longer oligomer. In the case of *n*βTE, absorption peak positions appeared in the UV region with a shoulder around 500 nm. In detail, 5βTE, 9βTE, and 13βTE showed absorption maxima at 313, 314, and 317 nm, respectively. The difference between the peak positions of 5βTE and 9βTE was 100 cm^{-1}, while the corresponding value of 5αTE and 9αTE was 1180 cm^{-1}. This fact indicates that *n*αTEs have highly extended π-electron systems, more than those of *n*βTE, because *n*αTE can take planar structure easily because of 2,5-bonding at the thiophene rings. In the case of *n*βTE, because the peak shift is also small for 13βTE, extension of π-conjugation seems to be limited. For the absorption band with similar shape, an increase in the extinction coefficients with an increase in the *n* value suggests that the limited π-conjugated units are linked without strong interaction in longer *n*βTEs. On the other hand, the red shift of the absorption edges and a slight broadening of the absorption

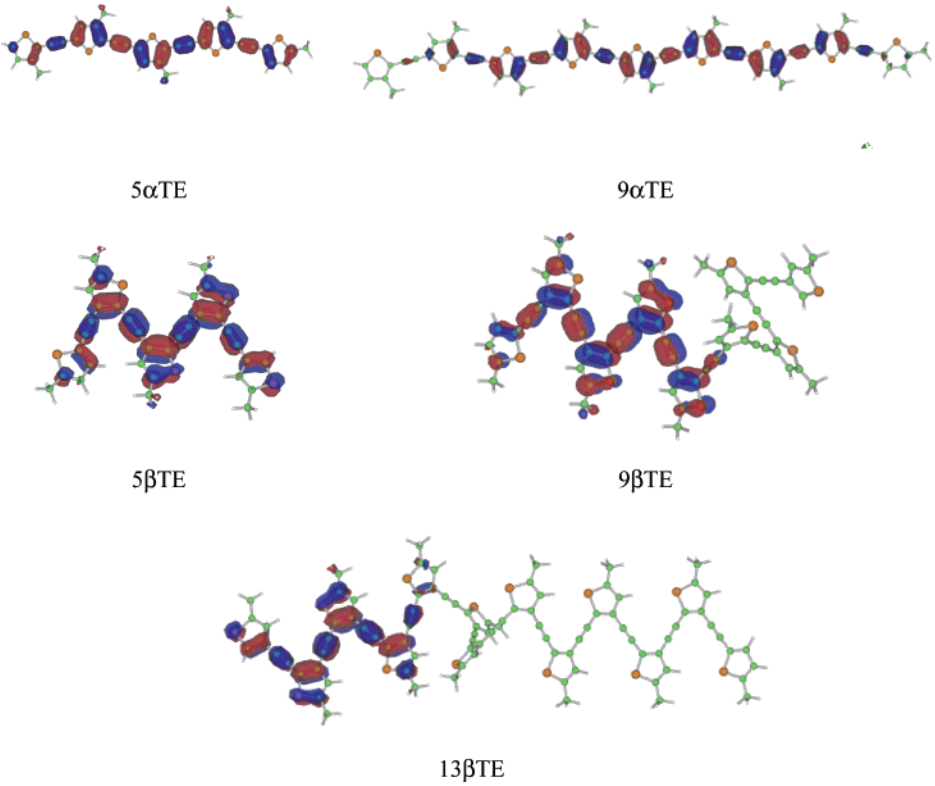

Figure 2. HOMO patterns of oligomers calculated at PM3 level.

peak of *n*βTE with an increase in the *n* value indicate that the expanded π-conjugation also slightly exists for longer oligomers. Thus, various structures with various degrees of the π-conjugations are expected for longer *n*βTE oligomers.

Theoretical calculation by the PM3 method indicates that 5αTE has a planar structure, which is favorable for extension of the π-conjugated system (Figure 2). Electron density of the HOMO state of 5αTE is extended all over the oligomer including thienylene and ethynylene moieties. Planar structure was also confirmed for 9αTE, although the π-conjugation is limited to the central seven thienylene−ethynylene units (Figure 2). This result is interesting from the point of view that various oligomers of π-conjugated polymers such as homo-oligothiophenes show saturations of various properties such as absorption and fluorescence peaks and redox properties around 6−8-mer.[3,14] Thus, the present result presents a new example of the theoretical indication for saturation of the π-conjugation in the oligomers of copolymer. In the case of 5βTE, planar structure and extended π-conjugation are also suggested (Figure 2). On the other hand, 9βTE has a folded structure: five planar thienylene−ethynylene units were connected with three units by one thiophene ring. Furthermore, 13βTE also has a folded structure composed of five thienylene−ethynylene units connected by three repeating units. The folded structures were also suggested by other calculations at AM1 level. Electron distributions of the HOMO states of 9βTE and 13βTE by PM3 were localized on one planar unit of the oligomers. Although the estimated structures for such longer oligomers should be regarded as one possibility, these findings explain well the spectral features of the steady-state absorption of *n*αTE and *n*βTE discussed above.

Electrochemical Properties. The oxidation potentials of *n*αTE and *n*βTE in benzonitrile were estimated by cyclic voltammetry as summarized in Table 1 (E_{ox}(*n*TE$^{\bullet+}$/*n*TE)). To avoid polymerization or degradation of the samples, the oxidation potentials were estimated from the first scan of the samples. In each case, an almost reversible oxidation wave was observed in the voltammogram. For both *n*αTE and *n*βTE, the lower oxidation potentials were observed with increasing number of the repeating units as reported for other oligomers of π-conjugated polymers. Thus, higher electron donor ability is expected for the longer oligomers.

Properties of Singlet Excited States of *n*αTE and *n*βTE. Upon excitation, *n*αTE and *n*βTE showed fluorescence bands around 500 nm accompanying shoulders as shown in Figure 1. In the cases of 5αTE and 9αTE, fluorescence maxima (λ_{max}-(S_1-S_0) in Table 1) appeared at 484 and 512 nm, respectively. Spectral shift between 5αTE and 9αTE was estimated to be 1130 cm^{-1}, which is almost the same as the shift observed in the steady-state absorption maxima. This fact indicates that the planar structures are maintained also in the singlet excited states of these oligomers. On the other hand, maxima of the fluorescence bands of 5βTE, 9βTE, and 13βTE are 449, 475, and 481 nm, respectively (Figure 1 and Table 1). The fluorescence peak shift between 5βTE and 9βTE was 1220 cm^{-1}, which is much larger than the steady-state absorption shift (100 cm^{-1}) and similar to the shift between 5αTE and 9αTE. This finding possibly indicates that the π-conjugation system of 9βTE in the singlet excited state has an expanded form like *n*αTE and 5βTE. Furthermore, the peak position of 13βTE shifted to red in comparison with 9βTE by 260 cm^{-1}. This shift of the fluorescence band of 13βTE indicates that the fluorescence of 13βTE also was generated from the expanded structure while the peak position change between 9βTE and 13βTE is small because of the "saturation" behavior of the longer oligomers.[3,14]

The fluorescence lifetimes (τ_F) of these oligomers were summarized in Table 1. The τ_F values of 5αTE and 9αTE are almost the same. Similar tendency was observed for *n*βTE oligomers. These results are adequate because the τ_F values of the homo-oligothiophenes become almost the same for the longer oligomer than pentamer, while τ_F values become longer with an increase in the number of the repeating unit for the shorter oligomer than pentamer.[3] The τ_F values of the oligo-

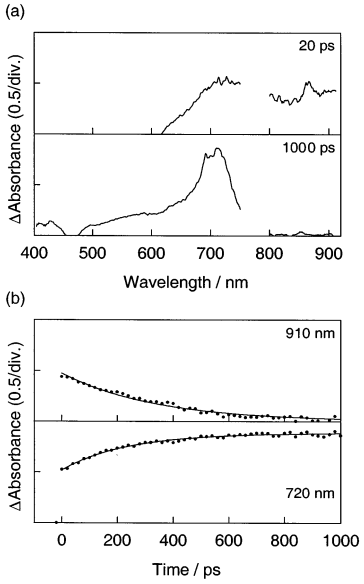

Figure 3. Transient absorption spectra (a) of 5αTE in toluene upon excitation at 388 nm (fwhm 150 fs) and (b) absorption−time profiles.

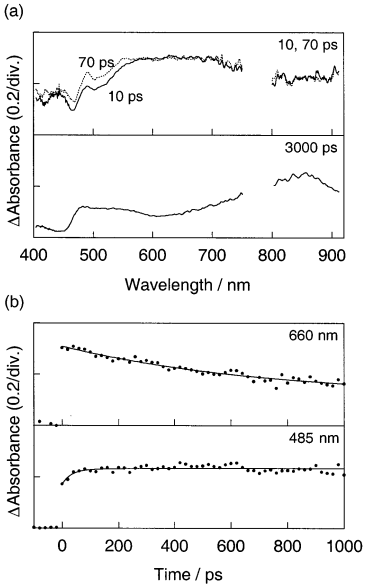

Figure 4. Transient absorption spectra (a) of 9*β*TE in toluene upon excitation at 388 nm (fwhm 150 fs) and (b) absorption−time profiles.

(thienylene−ethynylene)s in the present study do not show dependence on the number of the repeating unit because they are all larger than pentamer.

Transient absorption spectra of the singlet excited states of oligo(thienylene−ethynylene)s are investigated using femtosecond laser excitation at 388 nm. Upon excitation of 5αTE in toluene, transient absorption bands appeared at >900 and 720 nm (Figure 3a). The absorption band around 910 nm decayed with a decay rate constant of 3.0×10^9 s^{-1} (Figure 3b), which is almost the same as the fluorescence decay rate of 5αTE. Thus, it can be reasonably concluded that the absorption bands in longer wavelength than 700−920 nm are the singlet excited state of 5αTE. With the decay of the absorption band at >900 nm, the absorption intensity at 720 nm increased with the same rate constant as the decay at longer wavelength. Spectral feature at 1000 ps was different from that observed at 20 ps. These findings indicate that the transient spectrum at 1000 ps can be attributed to the triplet excited state of 5αTE, which is the same as the spectrum that was observed in the nanosecond laser flash photolysis discussed in a later section. Similarly, generation of the transient absorption bands of singlet excited states (λ_{max}-(S_1-S_n) in Table 1) and intersystem crossing processes were also confirmed for 9αTE and 5*β*TE.

In the case of 9*β*TE, a broad transient absorption band appeared around 660 nm at 10 ps after the laser irradiation (Figure 4a). In shorter time scale less than 100 ps, the absorption intensity at <500 nm showed an increase. At 3000 ps after the laser excitation, a new absorption band appeared around 840 nm with concomitant decay of the absorption band around 660 nm. The decay rate of the absorption band around 660 nm (1.4×10^9 s^{-1}) was almost the same as the fluorescence decay rate of 9*β*TE. Furthermore, the absorption band around 840 nm in the spectrum at 3000 ps can be attributed to the triplet excited state of 9*β*TE from the comparison with the nanosecond transient absorption spectra discussed later. From these findings, the respective decay and generation of the 660 and 840 nm bands can be attributed to the intersystem crossing process of 9*β*TE. The increase in the shorter time scale (<100 ps) cannot be attributed to the effect of the fluorescence because the rate constant of the increase of the absorption intensity was 3.2×10^{10} s^{-1}, which is much larger than the decay rate of the singlet excited state. In the previous section, the conformational change in the singlet excited state of 9*β*TE was suggested from the fluorescence properties. Thus, the possible explanation of the present spectral change in the shorter time region than 100 ps will be the conformational change, which induces extension of the π-electron system of 9*β*TE. This explanation seems to be adequate because 13*β*TE also showed the spectral change in the shorter time scale less than 100 ps after the laser excitation while 5*β*TE did not show such spectral change probably because of the planar structure of 5*β*TE in both the ground and excited states.

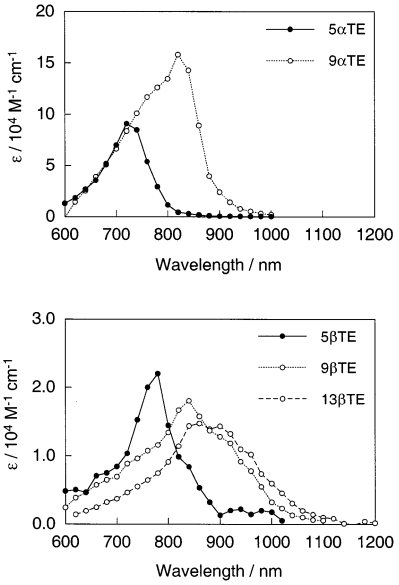

Figure 5. Transient absorption spectra of oligo(thienylene−ethynylene) in toluene at 100 ns after excitation with 355 nm laser (fwhm 6 ns).

Properties of Triplet Excited States of *n*αTE and *n*β*β*TE. Upon excitation with nanosecond laser pulse, 5αTE showed an absorption band at 720 nm (Figure 5), which can be attributed to the triplet excited state of 5αTE. This identification is supported by the fact that the absorption band was quenched in the presence of molecular oxygen, a typical triplet energy quencher. As shown in Figure 5, absorption bands of the triplet excited states were observed with other thienylene−ethynylene oligomers ($\lambda_{max}(T_1-T_n)$ in Table 1). In the cases of 5αTE and

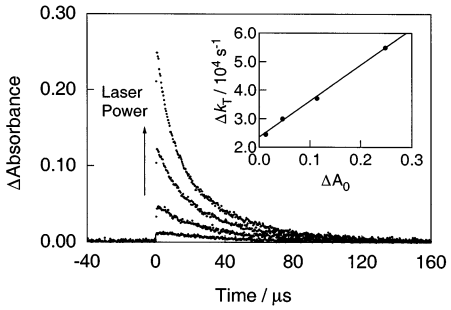

Figure 6. Laser power dependence of absorption time profiles of 5βTE in toluene at 780 nm. Inset shows the plot of initial decay rate (Δk_T) against initial absorbance (ΔA_0).

9αTE, the shift of the absorption peak and the increase in the extinction coefficient, which were estimated in the later section, were confirmed with an increase in number of the repeating unit. These features are the same as homo-oligothiophenes.[3] In the case of $n\beta$TE, the shift of the peak position was also confirmed, indicating that the expanded structures of longer $n\beta$TE in the singlet excited states seem to be retained also in the triplet excited states. Smaller extinction coefficients and the broad absorption bands perhaps indicate the contribution of various conjugation lengths in the triplet states due to various conformations.

The triplet absorption bands of the present oligomers decayed according to mixed order kinetics of first and second order (Figure 6), of which the contribution depends on the laser power, indicating that the triplet−triplet annihilation process (eq 1) exists in their triplet states.

$$^3n\text{TE}^* + {}^3n\text{TE}^* \xrightarrow{k_{TT}} {}^1n\text{TE}^* + n\text{TE} \qquad (1)$$

where k_{TT} is the rate constant for the triplet−triplet annihilation process. In eq 1, nTE denotes $n\alpha$TE or $n\beta$TE. The first- and second-order decay rate constants were estimated by using following relation (eq 2):

$$-\text{d}[\ln(\Delta A_{\text{initial}})]/\text{d}t = \Delta k_T = k_T^0 + (2k_{TT}/\epsilon_T)\Delta A_0 \qquad (2)$$

where $\Delta A_{\text{initial}}$, ΔA_0, and k_T^0 are absorbance change in initial part, T−T absorbance at $t = 0$, and an intrinsic decay rate of the triplet excited state of nTE ($1/\tau_T$, τ_T is an intrinsic triplet lifetime), respectively. As shown in an inset of Figure 6, plots of Δk_T against ΔA_0 show a linear relation. From the slope and the estimated ϵ_T value for 5βTE, the k_{TT} value was evaluated to be 1.4×10^9 M^{-1} s^{-1}, which is one-order smaller value than the diffusion-limiting rate of the solvent ($k_{\text{diff}} = 1.2 \times 10^{10}$ M^{-1} s^{-1} for toluene).[15] One-order smaller k_{TT} values than the k_{diff} value were also confirmed for other oligomers (Table 1). The k_{TT} values did not show the size and structure dependence. The present results are adequate for the planar structures in the excited triplet states; otherwise, the k_{TT} values of longer $n\beta$TE became small because of steric hindrance of nonconjugated part. As for τ_T values, which were on the same order with those of oligothiophenes, the size dependence was not observed.[3]

As indicated above, the triplet absorption bands of oligomers were quenched in the presence of oxygen. The quenching of the triplet absorption bands can be attributed to the energy-transfer process yielding the singlet oxygen (eq 3).

$$^3n\text{TE}^* + {}^3\text{O}_2 \xrightarrow{k_q(\text{O}_2)} n\text{TE} + {}^1\text{O}_2^* \qquad (3)$$

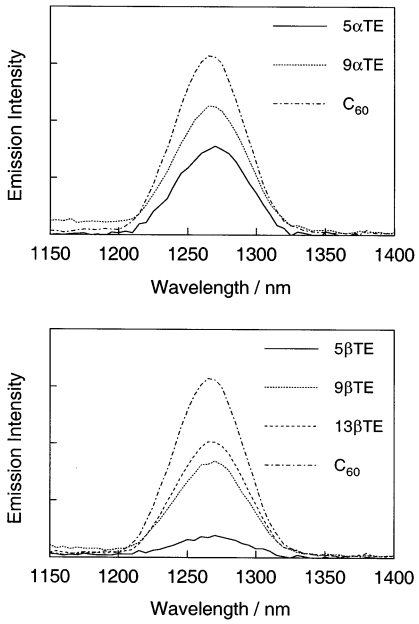

Figure 7. Emission spectra of singlet oxygen generated via (upper panel) 5αTE and 9αTE and (lower panel) 5βTE, 9βTE, and 13βTE in O_2-saturated toluene. Absorption intensities were matched at the excitation wavelength (514 nm).

The bimolecular quenching rate constant of the energy-transfer process ($k_q(O_2)$) was estimated to be 8×10^9 M^{-1} s^{-1} for 5αTE, indicating effective energy-transfer process. The generation of the singlet oxygen can be confirmed by observation of an emission band of the singlet oxygen at 1265 nm (Figure 7).[16] Emission spectra of singlet oxygen produced from the triplet states of the other oligomers are also shown in Figure 7 with C_{60} as a reference; the emission intensities were measured after the absorption intensities of the samples were matched at the excitation wavelength (514 nm). The emission intensities of the singlet oxygen via ^3nTE* are smaller than that via $^3C_{60}$*, indicating that the quantum yields for the triplet generation (i.e., Φ_{ISC}) of nTE are smaller than that of C_{60}. The quantum yield for the singlet oxygen generation ($\Phi_{^1O_2}$) can be expressed using the Φ_{ISC} value as eq 4:

$$\Phi_{^1O_2} = \Phi_{ISC}(k_q(O_2)[O_2]/(k_T + k_q(O_2)[O_2])) \qquad (4)$$

where k_T is the decay rate of the triplet absorption band in the absence of oxygen. The Φ_{ISC} values are listed in Table 1. The Φ_{ISC} values increased with the number of the repeating unit. This is an opposite feature to that reported for homo-oligothiophenes.[3] Furthermore, from the relative actinometry method using C_{60} as a standard,[17] extinction coefficients (ϵ_T) of the triplet excited oligomers were estimated as shown in Figure 5.

Radical Cation Formation by γ-Ray Irradiation. To confirm the spectral shapes of the radical cations of the oligomers, the γ-ray radiolysis experiments were carried out. The radical cations of the samples are expected to be generated via the hole transfer from the radical cation of *n*-butyl chloride formed by the γ-ray radiolysis.[8,18] Figure 8 shows the absorption spectra of the radical cations of $n\alpha$TE and $n\beta$TE. In the case of 5αTE, the absorption band appeared at 1800 and 740 nm (Table 1, $\lambda_{max}(n\text{TE}^{\bullet+})$), which will be attributed to the HOMO → SOMO and HOMO → LUMO transitions, respectively, as in the cases of the oligothiophenes[19] because the present oligomers have similar nondegenerated electron systems. For the radical cation of 9αTE, the absorption bands were at >2000 and 770 nm. The red shifts of the absorption bands indicate the extended

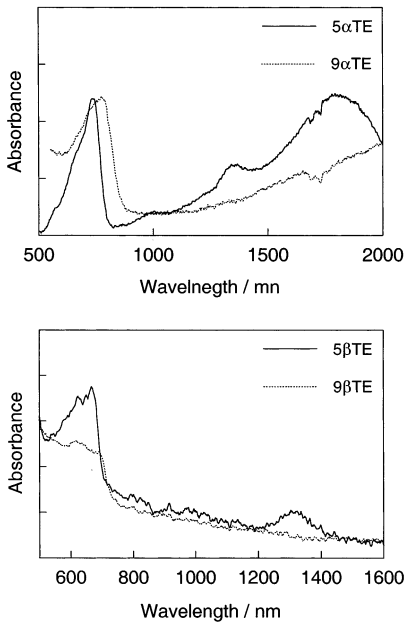

Figure 8. Absorption spectra of *n*TE in *n*-butyl chloride at 77 K upon γ-ray radiolysis.

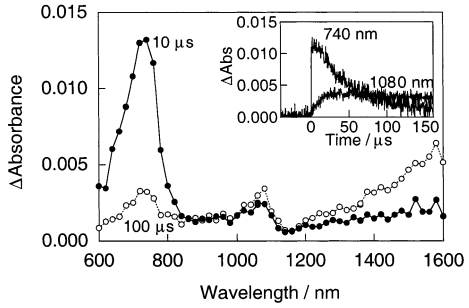

Figure 9. Transient absorption spectra of C_{60} (0.1 mM) in the presence of 5αTE (3.0 mM) upon excitation at 600 nm in benzonitrile. Inset shows the absorption−time profiles.

π-electron system of 9αTE even in the radical cation state. In the case of *n*βTE, observations of the absorption bands of the radical cations are difficult because of lower solubilities of *n*βTE in *n*-butyl chloride matrix at 77 K. For 5βTE and 9βTE, the radical cations showed the absorption bands at 668 and 688 nm, while substantial absorption bands due to the radical cation were not observed for 13βTE. The red shift of the absorption band is a similar trend as *n*αTE oligomers, indicating extended π-electron systems. In these cases, near-IR bands were not clear probably because of noisy spectra of low concentration samples.

Photoinduced Electron-Transfer Process with Fullerenes. From the oxidation potentials of the oligomers in the present study, they will act as electron donors in the presence of an appropriate electron acceptor upon photoexcitation. In the present study, we employed fullerenes (C_{60} and C_{70}) as electron acceptors because they show excellent acceptor abilities to oligothiophenes upon photoexcitation.[8c] In Figure 9, C_{60} was selectively excited by the 600 nm laser light in the presence of 5αTE in benzonitrile. An absorption band due to the triplet excited state of C_{60} ($^3C_{60}$*) appeared at 740 nm immediately after the laser pulse. At 100 μs after the laser, the absorption band due to $^3C_{60}$* decreased and new absorption bands appeared at >1600 and 1080 nm. The absorption band at 1080 nm can be attributed to the radical anion of C_{60}.[8c] The band at >1600 nm can be attributed to the radical cation of 5αTE from the comparison with the absorption spectra obtained by the γ-ray radiolysis (Figure 8). The absorption band at 740 nm of the radical cation of 5αTE is expected to be overlapped with the absorption band of $^3C_{60}$*. From the absorption time profiles at 1080 and 740 nm (inset of Figure 9), it was revealed that the radical anion of C_{60} ($C_{60}^{\bullet-}$) was generated with the concomitant decay of $^3C_{60}$*, indicating electron transfer from 5αTE to $^3C_{60}$* (eq 5):

$$^3C_{60}^* + n\text{TE} \xrightarrow{k_{ET}} C_{60}^{\bullet-} + n\text{TE}^{\bullet+} \quad (5)$$

In the present case, the possibility of two-electron transfer can be excluded because the formations of corresponding dication and dianion are not confirmed in the transient absorption spectra, although two-electron-transfer processes are reported for the longer oligomers in the electrochemical and chemical oxidation conditions.[10a,b]

It should be pointed out that the respective $^3C_{60}$* and $C_{60}^{\bullet-}$ showed decay and generation over several tens of microseconds. From the relation between the decay rate of $^3C_{60}$* and the concentration of 5αTE, the bimolecular quenching rate constant of $^3C_{60}$* (k_q) was estimated to be 2.5×10^7 M^{-1} s^{-1}, which is two orders smaller than the diffusion-limiting rate (5.3×10^9 M^{-1} s^{-1} in benzonitrile).[15] The quantum yield for electron transfer (Φ_{ET}) was estimated to be 0.28 from the ratio of the generated $C_{60}^{\bullet-}$ to the initially generated $^3C_{60}$*, indicating that other bimolecular quenching processes exist such as collisional quenching. The electron-transfer rate constant (k_{ET}) was estimated to be 7.0×10^6 M^{-1} s^{-1} from the relation, $k_{ET} = \Phi_{ET} k_q$. Similar electron-transfer processes with $^3C_{60}$* or $^3C_{70}$* were observed for other oligomers. The rate constants and quantum yields are summarized in Table 2, as well as the free-energy changes for electron transfer (ΔG_{ET}) estimated assuming an encounter distance to be 6 Å.[20] It was revealed that the k_{ET} values become larger for the longer oligomers for both *n*αTE and *n*βTE. This observation is adequate because the longer oligomers show higher donor ability as indicated by the low oxidation potentials.

In each electron-transfer system, the k_q and k_{ET} values are much smaller than the diffusion-limiting rate. The k_{ET} values were 0.07−0.0008 of the diffusion-limiting rate. These smaller rate constants cannot be explained on the basis of the ΔG_{ET} values because the ΔG_{ET} values are sufficiently negative values. The contribution of the energy-transfer process from triplet excited fullerene seems to be excluded because Φ_{ET} values increased for the longer oligomers, for which smaller triplet energies are expected, although we failed to observe phosphorescence of these oligomers probably because of quite weak

TABLE 2: Free-Energy Changes (ΔG_{ET} and ΔG_{BET}), Quenching Rate Constants (k_q), Quantum Yields (Φ_{ET}), and Electron-Transfer Rate Constants (k_{ET} and k_{BET}) for Forward- and Back-Electron-Transfer Process between Fullerenes and Oligo(thienylene−ethynylene)s in Benzonitrile

donor	acceptor	ΔG_{ET}[a,b]	k_q[c]	Φ_{ET}	k_{ET}[c]	ΔG_{BET}[a,b]	k_{BET}[c]
5αTE	$^3C_{60}$*	−2.54	0.25	0.28	0.070	−36.7	21
9αTE	$^3C_{60}$*	−4.15	0.23	0.42	0.10	−35.1	19
5βTE	$^3C_{60}$*	−2.54	0.16	0.27	0.043	−33.7	79
9βTE	$^3C_{60}$*	−5.29	3.3	0.40	1.3	−33.9	60
13βTE	$^3C_{60}$*	−6.00	3.7	0.62	2.3	−30.9	45
5αTE	$^3C_{70}$*	−3.46	0.23	0.49	0.11	−36.7	44
9αTE	$^3C_{70}$*	−5.07	1.5	0.63	0.95	−35.1	30
5βTE	$^3C_{70}$*	−3.36	0.75	0.54	0.41	−35.7	78
9βTE	$^3C_{70}$*	−6.23	3.3	0.64	2.1	−33.9	66
13βTE	$^3C_{70}$*	−6.92	5.1	0.74	3.8	−33.2	30

[a] In kcal M^{-1}. [b] Free-energy change was calculated assuming the encounter distance to be 6 Å. [c] In 10^8 M^{-1} s^{-1}.

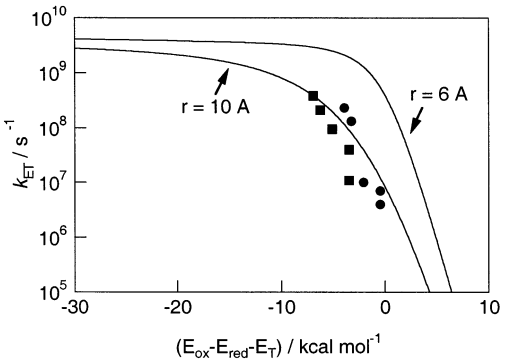

Figure 10. Relation between ($E_{ox} - E_{red} - E_T$) and k_{ET} of C_{60} (●) and C_{70} (■) with oligo(thienylene−ethynylene)s. Curves were estimated by assuming the distance of the encounter complex to be 6 or 10 Å from Rehm−Weller relation.

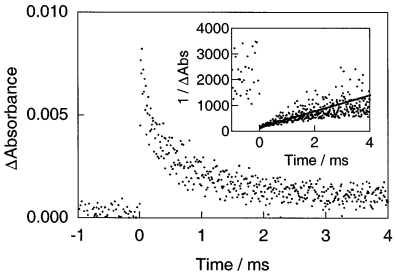

Figure 11. Absorption−time profile at 1080 nm of benzonitrile solution including C_{60} (0.1 mM) and 9αTE (3.0 mM) upon excitation at 600 nm. Inset shows the second-order plot.

phosphorescence as in the cases of the homo-oligothiophenes.[4,8] The smaller k_{ET} values for the present electron-transfer processes can be attributed to the longer distance in an encounter complex. In Figure 10, the k_{ET} values are plotted against the ($E_{ox} - E_{red} - E_T$) values, where E_{ox}, E_{red}, and E_T are oxidation potential of *n*TE, reduction potential of fullerene, and triplet energy of fullerene, respectively. The ($E_{ox} - E_{red} - E_T$) value corresponds to ΔG_{ET} without the Coulombic term in the Rehm−Weller relation.[20] As indicated in solid curves of Figure 10, the observed k_{ET} values are fitted well with the curve assuming that the encounter distance is to be 10 Å. The present findings indicate the long-range electron transfer due to the larger size of the oligomers and fullerenes. Similar long-range electron-transfer processes were reported for the fullerodendrimers.[21]

The generated radical ions decayed over several milliseconds as indicated in Figure 11 for C_{60} and 9αTE as a representative case. The decay of the radical ions can be attributed to the back-electron-transfer process (eq 6):

$$C_{60}^{\bullet -} + n\mathrm{TE}^{\bullet +} \xrightarrow{k_{BET}} C_{60} + n\mathrm{TE} \qquad (6)$$

As in the inset of Figure 11, the decay profile of the radical ions obeyed second-order kinetics, indicating that they exist as freely solvated radical ions rather than radical ion pairs because first-order kinetics is expected for the radical ion pair. From the slope of the second-order plot, the rate constant for the back-electron-transfer process (k_{BET}) from $C_{60}^{\bullet -}$ to 9αTE$^{\bullet +}$ was estimated to be 1.9×10^9 M^{-1} s^{-1}, indicating that the back-electron-transfer process is almost a diffusion-controlled process. For other electron-transfer systems, back-electron-transfer processes were confirmed to be second-order kinetic processes, and the k_{BET} values are summarized in Table 2. Although the k_{BET} values show slight scattering due to weak signal, all k_{BET} values are close to the diffusion-limiting rate constant. Such k_{BET} values are adequate because the free-energy changes for the back-electron-transfer processes (ΔG_{BET}) are sufficiently negative values to achieve the diffusion-limiting processes, even though the long-range electron-transfer processes are also expected for the present back electron transfer.

Conclusion

In the present study, two series of oligo(thienylene−ethynylene) show different properties depending on their conformations induced by 2,3- or 2,5-bonding at the thiophene rings. For *n*αTE, the expanded π-conjugated systems were indicated in the ground and excited states. Although the ground-state properties of *n*βTE were attributed to the limited π-conjugation system, the expanded π-conjugation was suggested in the excited state as *n*αTE. These findings are interesting from the view of application to molecular devices such as photochromism or photoactuator. Furthermore, donor abilities of the present oligomers were examined in the photoinduced electron-transfer processes with fullerenes (C_{60} and C_{70}). Slow electron-transfer rate constants of the present oligomers indicate long-range electron-transfer processes due to the larger size of the oligomers and fullerenes.

Acknowledgment. In the present work, the γ-ray radiolysis experiments were carried out at Tohoku University Cobalt 60 γ-ray Irradiation Facility. The present work was partly supported by a Grant-in-Aid on Scientific Research from the Ministry of Education, Science, Sports and Culture of Japan. The authors are also grateful to financial supports by Core Research for Evolutional Science and Technology (CREST) of Japan Science and Technology Corporation and The Mitsubishi Foundation. One of the authors (M.F.) thanks The Kao Foundation For Arts and Sciences for financial support.

References and Notes

(1) For recent reviews, see: (a) Tour, J. M. *Adv. Mater.* **1994**, *6*, 190. (b) Tour, J. M. *Chem. Rev.* **1996**, *96*, 537. (c) Marting, R. E.; Diederich, F. *Angew. Chem., Int. Ed.* **1999**, *38*, 1350. (d) Tour, J. M. *Acc. Chem. Res.* **2000**, *33*, 791.

(2) (a) Otsubo, T.; Aso, Y.; Takimiya, K. *Bull. Chem. Soc. Jpn.* **2001**, *74*, 1789. (b) Otsubo, T.; Aso, Y.; Takimiya, K. *J. Mater. Chem.* **2002**, *12*, 2565.

(3) (a) Becker, R. S.; de Melo, J. S.; Maçanita, A. L.; Elisei, F. *Pure Appl. Chem.* **1995**, *67*, 9. (b) Becker, R. S.; de Melo, J. S.; Maçanita, A. L.; Elisei, F. *J. Phys. Chem.* **1996**, *100*, 18683.

(4) (a) Scaiano, J. C.; Evans, C.; Arnason, J. T. *J. Photochem. Photobiol., B: Biol.* **1989**, *3*, 411. (b) Evans, C. H.; Scaiano, J. C. *J. Am. Chem. Soc.* **1990**, *112*, 2694.

(5) Wintgens, V.; Valat, P.; Garnier, F. *J. Phys. Chem.* **1994**, *98*, 228.

(6) Poplawski, J.; Ehrenfreund, E.; Cornil, J.; Bredas, J. L.; Pugh, R.; Ibrahim, M.; Frank, A. J. *Synth. Met.* **1995**, *69*, 401.

(7) (a) Sariciftci, N. S.; Smilowitz, L.; Heeger, A. J.; Wudl, F. *Science* **1992**, *258*, 1474. (b) Smilowitz, L.; Sariciftci, N. S.; Wu, R.; Gettinger, C.; Heeger, A. J.; Wudl, F. *Phys. Rev. B* **1993**, *47*, 13835. (c) Janssen, R. A. J.; Moses, D.; Sariciftci, N. S. *J. Chem. Phys.* **1994**, *101*, 9519. (d) Janssen, R. A. J.; Christiaans, M. P. T.; Pakbaz, K.; Moses, D.; Hummelen, J. C.; Sariciftci, N. S. *J. Chem. Phys.* **1995**, *102*, 2628.

(8) (a) Fujitsuka, M.; Sato, T.; Shimidzu, T.; Watanabe, A.; Ito, O. *J. Phys. Chem. A* **1997**, *101*, 1056. (b) Fujitsuka, M.; Sato, T.; Sezaki, F.; Tanaka, K.; Watanabe, A.; Ito, O. *J. Chem. Soc., Faraday Trans.* **1998**, *94*, 3331. (c) Matsumoto, K.; Fujitsuka, M.; Sato, T.; Onodera, S.; Ito, O. *J. Phys. Chem. B* **2000**, *104*, 11632.

(9) (a) Charra, F.; Fichou, D.; Numzi, J. M.; Pfeffer, N. *Chem. Phys. Lett.* **1992**, *192*, 566. (b) Lap, D. V.; Grebner, D.; Rehtsch, S.; Naarmann, H. *Chem. Phys. Lett.* **1993**, *211*, 135. (c) Lanzani, G.; Nisoli, M.; Magni, V.; De Silvestri, S.; Barbarella, G.; Zambianchi, M.; Tubino, R. *Phys. Rev. B* **1995**, *51*, 13770. (d) Lap, D. V.; Grebner, D.; Rentsch, S. *J. Phys. Chem. A* **1997**, *101*, 107.

(10) (a) Elandaloussi, E. H.; Frére, P.; Richomme, P.; Orduna, J.; Garin, J.; Roncali, J. *J. Am. Chem. Soc.* **1997**, *119*, 10774. (b) Jestin, I.; Frére, P.; Mercier, N.; Levillain, E.; Stievenard, D.; Roncali, J. *J. Am. Chem. Soc.*

1998, *120*, 8150. (c) Audebert, P.; Catel, J.-M.; Le Coustumer, G.; Duchenet, V.; Hapiot, P. *J. Phys. Chem. B* **1998**, *102*, 8661.

(11) (a) Tour, J. M. *Chem. Rev.* **1996**, *96*, 537. (b) Obara, Y.; Takimiya, K.; Aso, Y.; Otsubo, T. *Tetrahedron Lett.* **2001**, *42*, 6877. (c) Aso, Y.; Obara, Y.; Okai, T.; Nishiguchi, S.; Otsubo, T. *Mol. Cryst. Liq. Cryst.* **2002**, *376*, 153.

(12) Fujitsuka, M.; Masuhara, A.; Kasai, H.; Oikawa, H.; Nakanishi, H.; Yamashiro, T.; Aso, Y.; Otsubo, T. *J. Phys. Chem. B* **2001**, *104*, 9930.

(13) Frisch, M. J.; Trucks, G. W.; Schlegel, H. B.; Scuseria, G. E.; Robb, M. A.; Cheeseman, J. R.; Zakrzewski, V. G.; Montgomery, J. A., Jr.; Stratmann, R. E.; Burant, J. C.; Dapprich, S.; Millam, J. M.; Daniels, A. D.; Kudin, K. N.; Strain, M. C.; Farkas, O.; Tomasi, J.; Barone, V.; Cossi, M.; Cammi, R.; Mennucci, B.; Pomelli, C.; Adamo, C.; Clifford, S.; Ochterski, J.; Petersson, G. A.; Ayala, P. Y.; Cui, Q.; Morokuma, K.; Malick, D. K.; Rabuck, A. D.; Raghavachari, K.; Foresman, J. B.; Cioslowski, J.; Ortiz, J. V.; Stefanov, B. B.; Liu, G.; Liashenko, A.; Piskorz, P.; Komaromi, I.; Gomperts, R.; Martin, R. L.; Fox, D. J.; Keith, T.; Al-Laham, M. A.; Peng, C. Y.; Nanayakkara, A.; Gonzalez, C.; Challacombe, M.; Gill, P. M. W.; Johnson, B. G.; Chen, W.; Wong, M. W.; Andres, J. L.; Head-Gordon, M.; Replogle, E. S.; Pople, J. A. *Gaussian 98*, revision A.7; Gaussian, Inc.: Pittsburgh, PA, 1998.

(14) For example: (a) Diaz, A. F.; Crowley, J.; Bargon, J.; Gardini, G. P.; Torrance, J. B. *J. Electroanal. Chem.* **1981**, *121*, 355. (b) Lahti, P. M.; Obrzut, J.; Karasz, F. E. *Macromolecules* **1987**, *20*, 2023.

(15) Murov, S. L.; Carmichael, I.; Hug, G. L. *Handbook of Photochemistry*, 2nd ed.; Marcel Dekker: New York, 1993.

(16) Parker, J. G.; Stanbro, W. D. *J. Am. Chem. Soc.* **1982**, *104*, 2067.

(17) Carmichael, I.; Hug, G. L. *J. Phys. Chem. Ref. Data* **1986**, *15*, 1.

(18) Shida, T. *Electronic Absorption Spectra of Radical Ions*; Elsevier: Amsterdam, 1988.

(19) Fichou, D.; Horowitz, G.; Xu, B.; Garnier, F. *Synth. Met.* **1990**, *39*, 243.

(20) Rehm, D.; Weller, A. *Isr. J. Chem.* **1970**, *8*, 259.

(21) Kunieda, R.; Fujitsuka, M.; Ito, O.; Ito, M.; Murata, Y.; Komatsu, K. *J. Phys. Chem. B* **2002**, *106*, 7193.